

HIGH PRESSURE METAMORPHIC CONDITIONS IN GARNET AMPHIBOLITE FROM A COLLISIONAL SHEAR ZONE RELATED TO THE TAPU ULTRAMAFIC BODY, EASTERN CORDILLERA OF CENTRAL PERU

Arne P. Willner⁽¹⁾, Ricardo Castroviejo⁽²⁾, José F. Rodrigues⁽³⁾, Jorge Acosta⁽⁴⁾, Miguel Rivera⁽⁵⁾

⁽¹⁾ Institut für Geologie, Mineralogie und Geophysik, Ruhr-Universität, 44780 Bochum, Germany, arne.willner@rub.de; ⁽²⁾ Universidad Politécnica de Madrid, ETSI Minas, c/ Ríos Rosas, 21, 28003_Madrid, ricardo.castroviejo@upm.es; ⁽³⁾ Fac. Engenharia Univ. Porto (FEUP), r. Dr. Roberto Frias s/n 4200-465 Porto, Portugal, felic@fe.up.pt; ⁽⁴⁾ INGEMMET, Dirección de Recursos Minerales y Energéticos. Av. Canadá 1470. Lima 41- Perú. jacosta@ingemmet.gob.pe; ⁽⁵⁾ Miguel Rivera Feijóo, Av. Dos de Mayo 1312-503, Lima 27; mrivera@mineral-r.com.

INTRODUCTION AND SETTING

A discontinuous belt of elongated ultramafic rock bodies (mostly serpentinites) occurs in the Eastern Cordillera of the central Peruvian Andes. One of the main occurrences is the Tapo Massif, a lense-shaped serpentinite body, ~2 km x 5 km, comprising small podiform chromitite deposits (Castroviejo et al., 2009) and bands or lenses of garnet-amphibolite, both strongly sheared and thrust upon the upper Paleozoic sediments of the Ambo Group (Fig. 1). Metabasite geochemistry suggests a mid-ocean ridge or an ocean island protolith. The whole sequence can be interpreted as a disrupted ophiolitic complex (Castroviejo et al., 2010). The geological setting of the Tapo occurrence is described by J.F. Rodrigues et al. (2010). To get information about its geotectonic setting we applied new geothermobarometric techniques to the garnet amphibolite. Finding representative samples with an adequate mineralogy to apply these techniques is in this case a difficult task. A common problem is the almost ubiquitous overprinting by serpentinisation or retrograde metamorphism and, locally, by metasomatism or alteration enhanced by deformation, producing a variety of rock types, as rodingites, birbirites and listvaenites. Nevertheless, careful sampling followed by petrographic examination of the rocks allowed to identify some samples in which useful assemblages are present.

ASSEMBLAGES AND MINERAL CHEMISTRY

We selected three garnet amphibolite samples¹ (090606-2, 090606-3 and 270607-7, Fig. 1) which contain the assemblage garnet-Ca-amphibole-epidote-chlorite-albite-quartz-titanite-ilmenite. Additionally clinopyroxene is present in sample 090606-3. This assemblage points to conditions of the albite-epidote amphibolite facies.

Garnet is essentially an almandine-grossular solid solution (almandine_{0.46-0.62}grossular_{0.25-0.45}pyrope_{0.01-0.18}spessartite_{0.02-0.11}). Almandine and pyrope contents increase from core to rim, whereas spessartite decreases and grossular contents show little variations. Amphibole compositions vary strongly between samples: in sample 090606-3 amphibole is actinolite to magnesiohornblende (Na_A 0.10-0.66 apfu, Na_A 0.0-0.66 apfu, X_{Mg} 0.42-0.68), in sample 270607-7 magnesiohornblende to tschermakite (Na 0.58-1.03 apfu, Na_A 0.36-0.82 apfu, X_{Mg} 0.25-0.46) and in sample 090606-2 tschermakitic hornblende to tschermakite (Na 0.05-0.80 apfu, Na_A 0.3-0.5 apfu, X_{Mg} 0.41-0.58). Epidote composition within all samples varies strongly (X_{pistacite}=0.4-0.9) contrasting that of chlorite (Si 5.3-5.7 apfu; X_{Mg} 0.35-0.51). Clinopyroxene composition is diopside_{0.56-0.58}hedenbergite_{0.20-0.30}acmite_{0.07-0.10}orthopyroxene_{0.02-0.05}tschermak component_{0.02-0.07}. Plagioclase is invariably albite.

GEO-THERMOBAROMETRY

We calculated pseudosections for the three metabasite samples using the PERPLE_X software package (Connolly 2005). The thermodynamic data set of Holland & Powell (1998, updated 2002) for minerals and aqueous fluid was used. Calculations were performed using the following solid-solution models: for epidote, garnet, plagioclase, clinopyroxene, omphacite, amphibole and chlorite by Holland

& Powell (2003) and Powell & Holland (1999). For the calculation of the pseudosections the major element compositions analysed by XRF were simplified to a 9-component system (SiO₂-TiO₂-Al₂O₃-FeO-MgO-CaO-Na₂O-H₂O-O₂) normalized to 100% (Table 1). Water contents were augmented to excess water conditions that are considered to have prevailed during peak PT-conditions. Oxygen contents were arbitrarily chosen to account for epidote and Fe³⁺-rich clinopyroxene present in the samples. Calculated compositions of minerals provide good coincidence with measured ones (Table 2) except partly for amphibole, because solid solution models for amphibole are still not optimal.

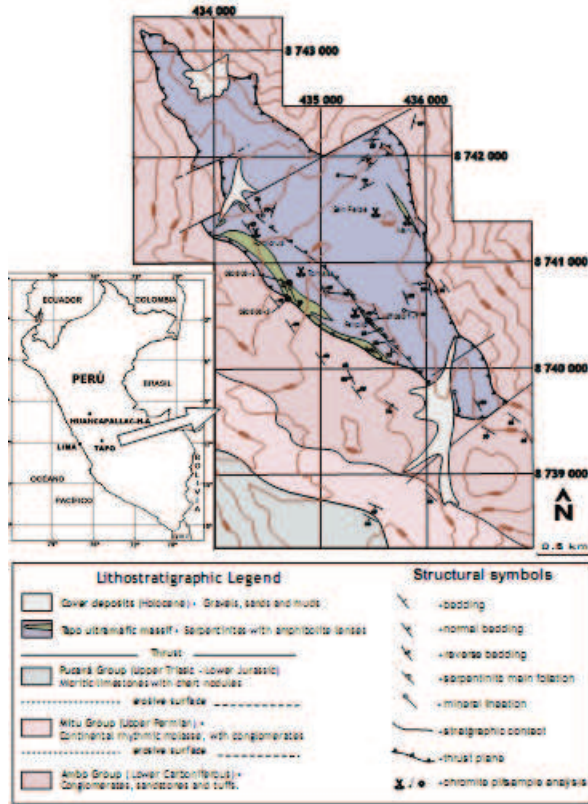


Fig.1. Geological map of the Tapo Ultramafic Complex with indications of the sample localities.

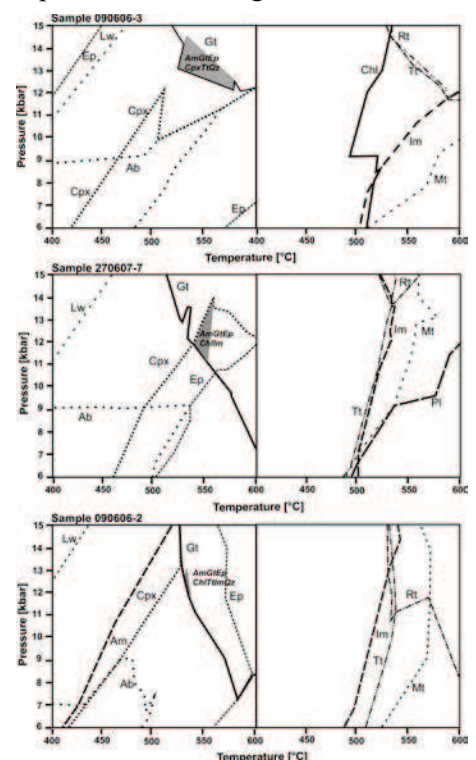
We simplified the pseudosections to present mere stability fields in the PT-range 400-600°C, 6-15 kbar in Fig.2. Garnet appears in the metabasite at conditions exceeding 8 kbar and 520°C. Whereas chlorite, epidote and Ca-amphibole are mostly stable in the considered PT-range, titanite is replaced at temperatures >520°C by ilmenite or rutile (>10 kbar). Albite is stable up to 520°C, 9 kbar and is partly replaced by plagioclase at higher temperature. Fe³⁺-rich clinopyroxene is stable up to about 7 kbar, 450°C and 12 kbar, 550°C, whereas omphacite was not formed under the considered conditions and compositions according to our calculation.

The assemblages representing peak metamorphic conditions coincide for all three selected samples within a range of 525-575°C,

11-14
kbar,
more

restricted for sample 090606-2 at 12-13 kbar, 530-540°C. Chlorite, albite and ilmenite are considered as retrograde phases in sample 090606-3, as albite, quartz and titanite in sample 270607-7 and albite in sample 090606-2.

Fig.2 Stability fields of minerals deduced from PT-pseudosections calculated from whole rock compositions (Table 1) in the system SiO₂-TiO₂-Al₂O₃-FeO-MgO-CaO-Na₂O-H₂O-O₂. Grey fields represent the stability field of the assemblages in the respective samples which represent peak PT-conditions. Abbreviations: Ab-albite, Am-Ca-amphibole, Chl-chlorite, Cpx-clinopyroxene, Ep-epidote, Gt-garnet, Im-ilmenite, Lw-lawsonite, Mt-magnetite, Pl-plagioclase, Rt-rutile, Tt-titanite.



CONCLUSIONS

We can restrict the peak metamorphic conditions for the Tapo Ultramafic Complex to 12.5 ± 1 kbar and $535 \pm 20^\circ\text{C}$ corresponding to 41-48 km burial depth (calculating with a mean crustal density of 2.8 g/ccm) and a low metamorphic geotherm of $10\text{-}13^\circ\text{C}/\text{km}$. Such conditions occur in subduction settings and collisional belts. Similar conditions were derived e.g. by Massonne & Calderón (2008) in a Devonian collision zone between an exotic microplate (“Chilenia”) and the South America. A comparable situation might also be conceivable for the situation in the Eastern Cordillera of Peru.

REFERENCES

- Castroviejo R et al. (2009) Proc. 10th. Biennial SGA Meeting, Townsville, Australia: 927-929.
 Castroviejo R et al. (2010) *Ophiolites in the Eastern Cordillera of the central peruvian Andes. IMA2010: 20th General Meeting of the International Mineralogical Association* (in press)
 Connolly JAD (2005) *Earth and Planetary Science Letters* 236: 524-541.
 Holland TJB, Powell R (1998) *Journal of Metamorphic Geology* 16: 309-343.
 Holland TJB, Powell R (2003) *Contributions to Mineralogy and Petrology* 145: 492-501.
 Massonne HJ, Calderón M (2008) *Revista Geologica de Chile* 35: 215-231.
 Powell R, Holland TJB (1999) *American Mineralogist* 84, 1-14
 Rodrigues JF et al. (2010) *Geología y Estructura de las Ultramafitas de Tapo y Acobamba (Tarma, Perú). Removilización tectónica andina de un segmento ofiolítico pre-andino.* (This vol.)

TABLE 1

(a) Whole rock compositions of metabasite				(b) Simplified compositions used for calculations of the pseudosections			
	090606-3	090606-2	270607-7		090606-3	090606-2	270607-7
(wt-%) SiO₂	49,43	40,01	40,35	(wt-%) SiO₂	47,28	41,51	39,30
Al₂O₃	11,55	10,11	10,99	Al₂O₃	11,05	10,49	10,70
Fe₂O₃	14,13	21,86	23,35	FeO	12,18	20,43	20,49
MnO	0,15	0,18	0,25	MnO	0,14	0,19	0,24
CaO	10,84	8,11	8,88	CaO	10,37	8,41	8,65
MgO	6,80	7,96	6,82	MgO	6,50	8,26	6,65
Na₂O	3,06	0,22	1,97	Na₂O	2,93	0,23	1,92
K₂O	0,12	0,06	0,12	TiO₂	2,46	3,38	4,95
TiO₂	2,57	3,26	5,09	H₂O	7,00	7,00	7,00
P₂O₃	0,13	0,01	<0.050	O₂	0,10	0,10	0,10
LOI	1,03	8,03	2,18	Sum	100,00	100,00	100,00
Sum	99,81	99,81	99,99				

Table 2 Representative mineral analyses and mineral compositions calculated with PERPLE_X for comparison

Clns.	090606	090606	Gross	090606	090606	090606	090606	090606	270607	270607	270607	Amphib	270607	270607	090606	090606	090606	090606
	-3	-3		-3c	-3r	-3	-2r	-2	-7c	-7r	-7		-7	-7	-2	-2	-3	-3
EPIDIOITE												calc						
SiO2	50.50	calc	SiO2	34.34	34.73	calc	38.29	calc	34.44	34.14	calc	SiO2	40.43	calc	44.29	calc	32.70	calc
Al2O3	1.43	533 C/ 13.15 Hex	Al2O3	21.04	21.04	533 C/ 13.15 Hex	21.75	533 C/ 13.35 Hex	21.07	21.11	540 C/ 11.90 Hex	Al2O3	14.18	540 C/ 11.90 Hex	9.57	533 C/ 13.35 Hex	3.47	533 C/ 13.15 Hex
TiO2	0.17		TiO2	0.15	0.15		0.04		0.17	0.12		TiO2	0.23		0.18		0.05	13.17H
Fe2O3	3.54		Fe2O3	0.50	0.53		0.00		0.42	0.99		Fe2O3	4.94		4.47		3.21	
FeO	7.14		FeO	21.28	21.42		22.85		25.42	24.24		FeO	20.14		13.59		12.77	
MnO	0.09		MnO	4.39	0.94		0.20		4.84	2.27		MnO	4.49		9.79		13.52	
MgO	11.84		MgO	0.32	1.13		0.47		0.35	0.31		CaO	10.59		10.24		11.75	
CaO	24.14		CaO	14.26	14.18		14.11		10.75	11.17		BaO	0.00		0.01		0.02	
H2O	0.34		Sum	98.38	98.34		100.52		99.48	99.70		K2O	0.23		0.07		0.05	
Sum	99.74		Si	5.891	5.918	4.000	4.000	4.000	5.892	5.844	4.000	H2O	3.03		1.75		0.37	
Si	1.921	2.000	Al	0.109	0.052		0.000		0.103	0.154		MnO	0.10		0.19		0.18	
Al	0.073		FeO	4.000	4.000		4.000		4.000	4.000		H2O	1.97		2.01		2.09	
FeO	1.994		Si	3.912	3.917	4.000	4.017	4.000	3.904	3.845	4.000	Sum	100.34		98.95		100.38	
Si	0.000	0.140	Fe3+	0.071	0.045		0.000		0.075	0.120		Si	4.204	7.144	4.891	7.540	7.57	7.521
Ti	0.005		Ti	0.018	0.018		0.007		0.021	0.015		Al	1.784	0.834	1.109	0.440	0.427	0.479
Fe3+	0.101		FeO	4.000	4.000		4.023		4.000	4.000		Sum	3.000	3.000	3.000	3.000	3.000	3.000
Fe2+	0.227	0.440	Fe2+	3.824	3.183	3.470	3.994	3.430	3.435	3.430	3.740	Si	0.755	0.984	0.570	0.420	0.194	1.259
Mn	0.003		Mn	0.403	0.128		0.104		0.443	0.311		Ti	0.027		0.020		0.004	
Mg	0.448	0.320	Ca	2.420	2.448	2.320	2.704	2.100	1.842	1.934	2.020	Mn	0.013		0.023		0.022	
Ca	0.978	0.340	Mg	0.078	0.272	0.230	0.177	0.220	0.024	0.194	0.240	Fe3+	0.549		0.523		0.248	
H2	0.025	0.140	FeO	4.044	4.032	4.000	5.941	4.000	4.044	4.071	4.000	Fe2+	2.570	2.190	1.492	2.080	1.535	1.300
FeO	2.004	2.000	Sum	0.012	0.011		0.000		0.012	0.020		Mg	1.047	1.823	2.172	2.190	2.894	1.941
O	4.000		Gross	0.399	0.395	0.387	0.454		0.294	0.299		Sum	13.000	13.000	13.000	13.000	13.000	13.000
Total	0.005		Spec	0.100	0.021		0.018		0.110	0.051		Ca	1.731	1.515	1.729	1.920	1.810	1.131
MgO	0.003		FeO	0.013	0.045	0.038	0.024		0.014	0.032		Ba	0.000		0.001		0.001	
Ti	0.048		AlO3	0.477	0.128	0.577	0.502		0.548	0.598		H2	0.910	0.790	0.504	0.200	0.243	0.940
Sum	0.101		Cations based on 48 negative charges including 10 cations in the tetrahedral and octahedral site to calculate Fe3+, c core, rrim.										K	0.044		0.013		0.009
Obs	0.047											Sum	2.484	2.305	2.244	2.120	2.043	2.091
Hex	0.197											OH	2.000	2.000	2.000	2.000	2.000	2.000
Dep	0.530		Chlorite	270607	270607	090606	090606	090606					Proportion of cation x based on the sum of cation = 13 except for Ca, H2 and K for summation of Fe3+ and on +4 as given charge					
XFe	0.253												270607	270607	090606	090606	090606	090606
XFe3	0.308												Epilote					
			SiO2	34.44	calc	35.85	calc	34.99				SiO2	38.14	calc	37.44	calc	37.98	calc
			Al2O3	17.90	540 C/ 11.90 Hex	20.34	533 C/ 13.35 Hex	19.53				Al2O3	28.18	540 C/ 11.90 Hex	28.33	533 C/ 13.35 Hex	22.53	533 C/ 13.15 Hex
			TiO2	0.07		0.02		0.01				Fe2O3	7.49		7.27		13.19	13.15 H
			FeO	31.99		28.45		28.41				Mn2O3	0.05		0.04		0.01	
			MgO	12.43		12.75		12.88				TiO2	0.11		0.10		0.09	
			MnO	0.35		0.34		0.38				CaO	23.79		23.32		23.48	
			CaO	0.15		0.04		0.03				H2O	1.91		1.87		1.90	
			H2O	0.07		0.00		0.00				Sum	99.94		98.41		100.44	
			H2O	11.18		11.22		10.98				Si	3.000	3.000	3.000	3.000	3.000	3.000
			Sum	100.40		99.27		97.52				Al	2.411	2.320	2.474	2.400	2.190	2.520
			Si	5.475	5.940	5.524	5.940	5.459				Ti	0.004		0.004		0.005	
			Al	2.325	2.040	2.474	2.040	2.541				Mn	0.003		0.002		0.001	
			Si	3.203	2.040	2.452	2.040	2.503				Fe	0.455	0.450	0.438	0.400	0.784	
			Ti	0.012		0.003		0.001				Sum	3.074	3.000	3.122	3.000	2.981	0.450
			Mn	0.044		0.042		0.070				Ca	2.003	2.000	2.001	2.000	2.004	3.000
			Fe	5.743	5.960	5.120	5.740	5.228				Sum	2.005		2.001		2.008	
			Mg	3.979	3.960	4.055	4.220	4.197				OH	1.000	1.000	1.000	1.000	1.000	1.000
			Sum	12.000	12.000	11.891	12.000	11.999				O	12.123	12.000	12.187	12.000	11.980	12.000
			H2	0.028		0.000		0.000				Proportion of cation x based on normalization of 36 base cation						
			Ca	0.024		0.014		0.018										
			OH	14.000	14.000	14.000	14.000	14.000										